Fuel 297 (2021) 120607

Contents lists available at ScienceDirect

Fuel

journal homepage: www.elsevier.com/locate/fuel

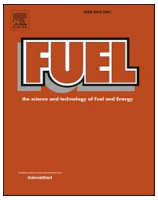

Full Length Article

A novel technique for interface analysis: Behaviour of sophorolipids biosurfactant obtained from *Meyerozyma* spp. MF138126 during low-salinity heavy-crude experiments

Lateef T. Akanji [a,*], Ramla Rehman [b], Chibuzo C. Onyemara [a], Rainer Ebel [c], Asif Jamal [b]

[a] School of Engineering, University of Aberdeen, Aberdeen AB24 3FX, UK
[b] Department of Microbiology, Faculty of Biological Sciences, Quaid-i-Azam University, Islamabad 45320, Pakistan
[c] School of Natural and Computing Sciences, University of Aberdeen, Aberdeen AB24 3FX, UK

ARTICLE INFO

Keywords:
Interfacial phenomenon
HPHT
Anaerobic fermentation
Microbial EOR
Biosurfactant producing microbes
High-temperature cultivation
Low-salinity
Heavy-crude

ABSTRACT

A novel technique for interface behaviour and thermodynamic properties analyses of sophorolipids (SLs) biosurfactant obtained from *Meyerozyma* spp. MF138126 under high-pressure high-temperature (HPHT), for low-salinity heavy-crude experiments is presented. An experimental rig for production of biosurfactant and determination of interfacial tension (IFT) under HPHT is developed specially for the purpose of this investigation. A reduction of a factor of seven and nine in IFT was obtained for experiments between brine and heavy-crude at temperatures of 45°C and 65 °C respectively. Furthermore, with increasing temperature, the degree of SLs adsorption at the interface increases leading to a total collapse in the profiles of the adsorption graphs. The minimum area per molecule of SLs monomers for different conditions suggested that the interface weakens occupying more surface area as the temperature increases. The degree of counter-ion binding for SLs is obtained to be 0.86. The computed Gibbs free energy of micellisation is −1940 KJ/mol; which is exergonic depicting favourable reaction and spontaneous in forward direction. At a fixed temperature of 25 °C and pressure of 45 bar, IFT value of 0.251 mN/m was obtained. It is concluded that the produced SLs retained its molecular integrity and IFT reduction effectiveness under both unconfined and confined HPHT systems.

1. Introduction

Enhanced Oil recovery (EOR) is a tertiary method that improves the recovery of petroleum hydrocarbons from the reservoir after primary and secondary production phases. In recent years, variety of methods like thermal, chemical and miscible or solvent injection which involve the use of steam, surface active compounds and hydrocarbon gases, respectively, have been employed for EOR. Amongst the different types of surface active compounds, cationic and anionic surfactants are known to possess positively and negatively charged ions respectively; while amphoteric surfactants possess both positively and negatively charged ions [1]. The amphiphilic nature of surfactants make them readily able to dissociate in polar and non-polar fluids [2–4]. However, due to the environmental risks associated with the use of chemical surfactants and the possible high expenses, there is a need to develop alternative methods that are environmentally benign and also capable of enhancing oil recovery (e.g. Kiran et al. [5], Ramos et al. [6]). The surfactant solution will dissociate to form monomers at the initial stage, while the dissociated monomers will later aggregate at increasing concentration to form micelles commonly referred to as supramolecules [7].

Microbial EOR (MEOR) encompasses the use of microorganisms and their products to extract the remaining oil from reservoirs. Further, due to its green nature and eco-friendliness, MEOR is gaining considerable importance as it provides biotechnological solution to the problems of the petroleum industry (e.g. Al-Sulaimani et al. [8], Chisholm et al. [9], Budiharjo et al. [10]). MEOR can be achieved either by insitu injection of microorganisms or by the mass flooding of nutrients, biosurfactants, biopolymers, biologically produced acids, gases and solvents into the reservoir (e.g. Poremba et al. [11]). We advocate ex-situ production of biosurfactant where interfacial adsorption and thermodynamic properties are critically evaluated prior to utilisation. The thermodynamic standard Gibbs free energy required for the formation of SLs; a type of glycolipids obtained from the strain of *Meyerozyma*, which can be used in the prediction of the degree of spontaneity, surface adsorption, surface affinity and binding potentials, critical micelle concentration (CMC)

* Corresponding author.
E-mail address: l.akanji@abdn.ac.uk (L.T. Akanji).

https://doi.org/10.1016/j.fuel.2021.120607
Received 6 April 2020; Received in revised form 28 February 2021; Accepted 1 March 2021
Available online 10 April 2021

Nomenclature

Nomenclature

P	= pressure, Pa
T	= temperature, °C
ρ	= density, g/cm^3
M	= molecular weight, g/mol
g	= acceleration due to gravity, m/s^2
R_0	= radius of curvature at the drop apex
β	= shape factor
θ	= angle, °
V	= volume, cm^3
D	= diameter of pendant drop, cm
ν	= ratio of diameters of a drop
H	= drop height, cm
μ	= fluid viscosity, cp
B	= transformed shape parameter
γ	= IFT or ST, mN/m
Γ	= surface excess concentration, mol/m^2
κ	= conductivity, mS/cm
ρ_e	= environmental phase density (g cm^{-3})
ρ_d	= drop-phase density (g cm^{-3})
R	= universal gas constant, 8.314 J/K mol
A_{min}	= minimum area per molecule of surfactant, cm^2
a	= activity
c	= concentration, mol/L

Acronyms

IFT	= interfacial tension
ST	= surface tension
HPHT	= high-pressure high-temperature
SLS	= sophorolipids
OD	= optical density
COBR	= crude oil/brine/rock
COBBIO	= crude oil/brine/biosurfactant
COBBIOR	= crude oil/brine/biosurfactant/rock
CMC	= critical micelle concentration
TDS	= total dissolved solid
mM	= milli-Molarity = 1 × 10^{-3} mol/L

aggregates formation in immiscible bulk water phase and rapid surface tension (ST) and IFT reduction property has never been studied or published to the best of our knowledge.

The mechanisms associated with adsorption of biosurfactants at the interfaces involve ion exchange where previously adsorbed counterions at the interface are replaced by similar but different ions from the bulk solution; ion-pairing in which surfactants are adsorbed on to free counterions from the solution; hydrogen bonding and Van der Waal dispersive forces [12–14]. Previous studies have demonstrated the application of some biosurfactants producing microorganisms in EOR related studies. This is mainly related to their ability to reduce the oil–water IFT (e.g. Al-Wahaibi et al. [15], Al-Araji et al. [16], Anitha and Jeyanthi [17]). However, adsorption of sophorolipids (SLs) at heavy crude oil-brine interface has not been established [18,19]. Most studies on adsorption of some other biosurfactants have been in medical, food sciences and environmental remediation [20].

Recently, some researchers have isolated yeast for the production of biosurfactant purposes. For instance, Camargo et al. [21] characterised and evaluated the capacity of yeast to produce biosurfactant under acidic conditions using soybean oil frying waste as the main source of carbon. Specific application was in bioremediation and metal removal processes in anaerobic sewage sludge. Under a similar application, Camargo et al. [22] investigated the influence of co-inoculation of Acidithiobacillus bacteria and the biosurfactant-producing yeast *Meyerozyma guilliermondii* in bioleaching processes. This study suggested that after 10 days of incubation, 76.5% of Zn, 59.8% of Ni, 22.0% of Cu, 9.8% of Cd, 9.8% Cr and 7.1% of Pb were solubilised with the presence of yeast contributing to the reduction in the time required for Cd to solubilise from 240 to 96 h.

Despite the recent advances in the production of biosurfactant from yeasts, application has only been limited to ambient conditions of low-pressure low-temperature (e.g. Liang et al. [23]) associated with environmental remediation processes. Ganji et al. [24] reported the production of sophorolipids from an isolated strain of Candida keroseneae under ambient condition and its possible use in MEOR. In another study, Elshafie et al. [25] conducted core flooding experiments using the SLs produced from a strain of Candida bombicola. For this purpose, the seed culture was incubated at room temperature. However, specific application in MEOR process under elevated insitu conditions is sparse. Further, microorganisms isolated for MEOR should endure high temperature, pressure and salinity and be capable of growth under anaerobic or microaerophilic conditions. Up till now, different strains of *Bacillus*, *Geobacillus*, *Pseudomonas*, *Rhodococcus*, *Clostridium*, *Mycobacterium* and *Brevibacterium* have been used in various in situ MEOR studies. However, the mechanisms underpinning the full spectrum of anaerobic fermentation, high-pressure high-temperature (HPHT) anaerobic cultivation, screening, physico-chemical analysis of SLs biosurfactant obtained from *Meyerozyma* spp. MF138126; prior to EOR applications, have not been previously investigated and are therefore not well understood.

One aspect of this work therefore involves development of a novel technique for the production of SLs biosurfactant under HPHT conditions on the one hand and evaluation of the interface behaviour of the produced SLs during low-salinity heavy-crude experiments on the other hand. The other aspect involves the development of an unconventional technique for interface analysis under HPHT insitu conditions. Conventional techniques involve coupling an image analysis package using video camera, data acquisition system and commercial algorithms for the measurement of the coordinates of the pendant drop to determine IFT or ST (e.g. Bagalkot et al. [26]). In this unconventional design setup, the IFT chamber has a design pressure and temperature of 500 MPa (5000 bar) and 175 °C respectively. Furthermore, the system also allows for both bubble and pendant drop experimental measurements to be carried in a single setup.

The potential of the newly isolated SLs producing microbial strain of *Meyerozyma* spp. MF138126 to increase recovery of heavy crude oil through surface and IFT reduction in a typical low formation salinity water is therefore investigated. In order to achieve this, a novel protocol for cultivation of previously optimised strains of *Meyerozyma* spp. MF138126 under elevated culture temperature and pressure is developed. It involves anaerobic fermentation under shake-flask experiments and then HPHT cultivation for the production of SLs from optimised *Meyerozyma* spp. MF138126. Samples are collected periodically under varying conditions of temperature and pressure to monitor growth-rate and produced cellular biomass using spectrophotometer. SLs is obtained through solvent extraction technique and the effect of HPHT conditions on their chemical structure was determined through Fourier-transform infrared spectroscopy (FTIR) analysis.

The economics of the application of SLs biosurfactant can be evaluated as part of crude oil/brine/biosurfactant/rock (COBBIOR) experimental analysis. In order to achieve a cost-effective EOR process, biosurfactant affinity to rock surface must be evaluated. Some of the critical COBR parameters include adsorption, precipitation and phase trapping. These parameters have a direct bearing on the porous system

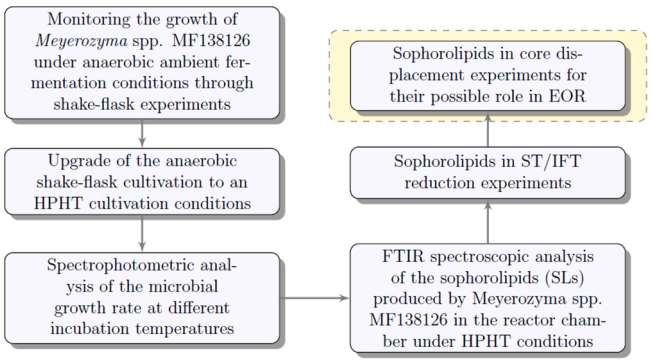

Fig. 1. Developed protocol for the microbial enhanced oil recovery process. Application of the produced SLs in core displacement or COBBIOR experiments (as highlighted in yellow) is outside the scope of this investigation.

Table 1
Minimal salt medium (MSM) optimised for the production of sophorolipids from *Meyerozyma* sp. MF138126.

Media formulation	Quantity (g/L) or (%)	Unit
Glycerol	5	%
NaH_2PO_4	0.4	g/L
Peptone	10	g/L
Yeast extract	0.5	g/L
$MgSO_4$	0.1	g/L

temperature and salinity. A significant loss of surfactant may occur due to adsorption of biosurfactant on to the rock surfaces (e.g. Amirianshoja et al. [27] and Barati-Harooni et al. [28]). This may impact the overall cost of the process as well as the effectiveness of the surfactant in reducing IFT.

In this work, a series of crude oil/brine/biosurfactant (COBBIO) screening experiments involving ST and IFT measurements between typical formation brine and heavy-crude oil in unconfined and confined special purpose HPHT experimental rig is conducted. Adsorption is investigated as part of COBBIO IFT analyses. The thermodynamic behaviour of the SLs is further investigated as outlined in this paper where the tendency for SLs to maintain its structural integrity under reservoir brine system is also established. All data label prefixed by S can be found in the supplementary material. Application of the produced biosurfactant in actual core-flooding or COBBIOR experiment is outside the scope of this paper.

2. Materials and method

The new protocol developed for the purpose of this investigation is shown in Fig. 1. It consists of six (6) steps involving: (a) Anaerobic shake-flask cultivation of *Meyerozyma* spp. MF138126 under ambient pressure and temperature; (b) Anaerobic cultivation of *Meyerozyma* spp. MF138126 under HPHT by upgrading the shake-flasks cultivation; (c) Spectrophotometric analysis of the microbial growth rate at the two incubation temperatures i.e. 25 and 45 °C, provided in the reactor chamber (d) FTIR spectroscopic analysis of the SLs produced under HPHT conditions; (e) SLs in ST/IFT reduction experiments; (f) SLs in core displacement experiments for possible role in EOR. Each step involved in the protocol is explained further below. Step (f) is beyond the scope of this investigation.

2.1. Anaerobic cultivation of Meyerozyma spp. MF138126 under ambient conditions

The strain *Meyerozyma* spp. MF138126 was previously isolated from a crude oil contaminated site. It was then screened based on its morphological and molecular identity and screened in order to determine its SLs producing capabilities [29]. Anaerobic cultivation of the strain was done at lab-scale for a period of one week in a minimal salt medium (MSM) with the composition highlighted in Table 1. This was followed by the incubation of culture broth in 250 ml Erlenmeyer flasks at 37 °C and atmospheric pressure. Samples were taken from the culture flasks after every 24 h and the growth rate was monitored at 600 nm using a UV-visible spectrophotometer. All readings were taken in triplicates.

2.2. Anaerobic cultivation of Meyerozyma spp. MF138126 under HPHT conditions

Anaerobic cultivation of *Meyerozyma* spp. MF138126 was done under HPHT conditions. The HPHT anaerobic cultivation reactor (Fig. 2) allows a wide range of microbial fermentation processes to be carried-out under different pressure (designed to operate up to 200 bar) and temperature conditions (designed to operate up to 250 °C). The salient feature of this advanced rig includes source of imposed system pressure, automatic vent-gas system, digital pressure transducer, digital

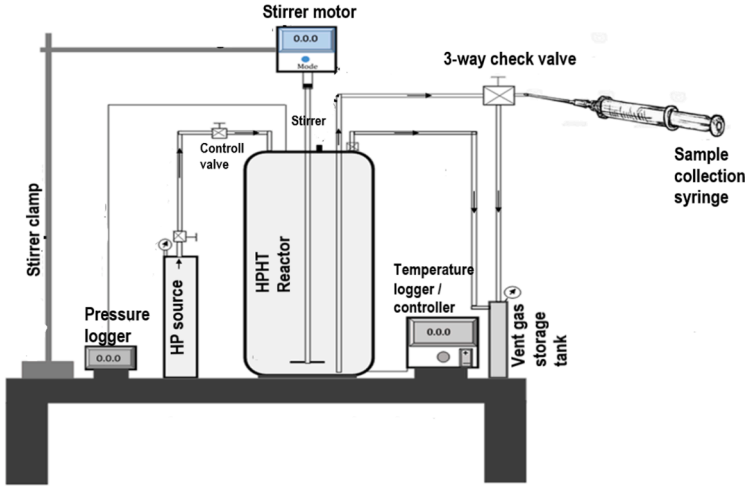

Fig. 2. HPHT reactor cell for the anaerobic cultivation of microbes. The features of this advanced rig includes source of imposed system pressure, automatic vent-gas system, digital pressure transducer, digital temperature monitoring system, pressure-relief valve, rupture disc and vent bio-gases storage tank with pressure indicator. Further details on the actual design of the system are available in another publication [30].

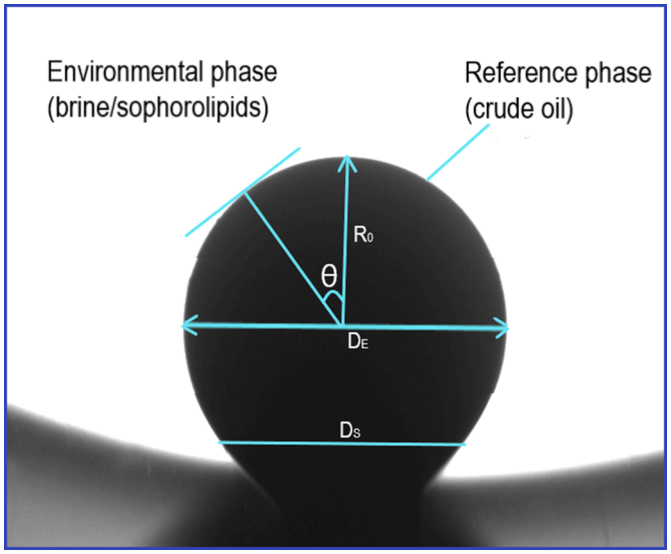

Fig. 3. Drop image formed by the reference phase (heavy-crude) in the environmental phase (brine/sophorolipids aqeous solution).

temperature monitoring system, pressure-relief valve, rupture disc and vent bio-gases storage tank with pressure indicator. The system is specially configured to allow all produced bio-gases by the microorganisms to be captured and discharged in a pressure vessel.

Following the inoculation process, 800 ml of the culture broth was incubated in the reactor chamber of the rig. A pressure of 1 and 10 bar was supplied to the microbial culture at 25 °C for a period of 7 days in a sequential experiment. In the last phase of experiment, the temperature was elevated to 45 °C with the pressure kept constant. Samples were collected at periodic intervals with a syringe through a three-way check-valve. Growth rate was monitored by measuring the optical density of culture medium at 600 nm using a UV-visible spectrophotometer. All readings were taken in triplicates. Extraction of SLs is then carried out using solvents (Ethyl acetate, Methanol etc.) and chemical/molecular characterisation of SLs through different analytical techniques; such as Fourier-transform infrared spectroscopy (FTIR) and liquid chromatography mass-spectroscopy (LCMS) conducted.

2.3. FTIR spectroscopic analysis of the SLs produced under HPHT conditions

Post incubation at 25 and 45 °C, the culture broth was centrifuged at 10,000 rpm for 10 min to remove cell pellet. This was followed by the structural analysis of sophorolipids produced by *Meyerozyma* spp. MF138126 at the two incubation temperatures through FTIR spectroscopy.

2.4. Principle of IFT measurement

The pendant drop technique is a reliable and an effective method of measuring the IFT of liquid–gas or liquid–liquid system. The shape of the pendant drop (see Fig. 3) is governed by gravity and the ST/IFT [31]. The IFT is calculated from the shadow of the digital image captured by the video-camera using the drop shape analysis which relies on Young–Laplace equation:

$$\Delta P = \gamma \cdot \left(\frac{1}{r_1} + \frac{1}{r_2}\right), \tag{1}$$

where, ΔP is the pressure across the interface, r_1 and r_2 are the principal radii of the pendant drop, and γ is the ST/IFT.

Table 2
Typical low-salinity formation brine formulated and used in this investigation.

Material	Mass (mg)	Deionised water volume (ml)	Material MW (mg/mol)	Molarity (mg/l)
Sodium chloride (NaCl)	23740	1000	58440	0.40623
Potassium chloride (KCl)	755.0		74551.3	0.01013
Magnesium chloride hexahydrate ($MgCl_2.6H_2O$)	10700		203310	0.05263
Calcium chloride dihydrate ($CaCl_2.2H_2O$)	1500		147008	0.01020
Strontium chloride hexahydrate ($SrCl_2.6H_2O$)	24.00		266620	0.00009
Sodium sulfate (Na_2SO_4)	3976		142040	0.02799
Sodium bicarbonate ($NaHCO_3$)	194.0		84007	0.00231
Total dissolved solid (TDS) and brine stock molarity	40889			0.50958
Stock brine pH: 7.51				

$$\gamma = \frac{\Delta\rho g R_0^2}{\beta}, \tag{2}$$

where, $\Delta\rho$ is the mass density difference between the drop and the surrounding medium, g is the gravity constant, R_0 is the radius of curvature at the drop apex and β is the shape factor. By convention, $\Delta\rho$ is defined such that $\Delta\rho$ and β are negative for pendant drops and positive for sessile drops. For drops that are sufficiently long in order to measure the diameter D_S (i.e. pendant drops) the maximum diameter, D_E, and the ratio:

$$\nu = \frac{D_S}{D_E}. \tag{3}$$

β is then defined thus (see Hansen [31]):

$$\beta = -0.12836 + 0.7577\nu - 1.7713\nu^2 + 0.5426\nu^3 \tag{4}$$

$$\gamma = \frac{\Delta\rho g H^2}{B}, \tag{5}$$

where, B is a transformed shape parameter which may be derived from Eqs. 2 and 5 thus:

$$B = \beta \times \chi^2, \tag{6}$$

where, $\chi = \left(\frac{H}{R_0}\right)$, H is the drop height and R_0 is the radius of curvature at the drop apex. From Eqs. (1)–(6) above, it can be observed that with the exception of $\Delta\rho$, the size parameters R_0 and β are derived from the drop profile.

2.5. Application of SLs produced by Meyerozyma spp. MF138126 in ST and IFT analysis

In order to evaluate the effectiveness of the SLs (produced at the two incubation temperatures of 25 and 45 °C) in reducing ST and IFT, several measurements involving low-pressure low-temperature and low-pressure high-temperature were carried out. Furthermore, the role of crude SLs in interfacial phenomena was determined through special purpose rig assembly involving pendant drop method.

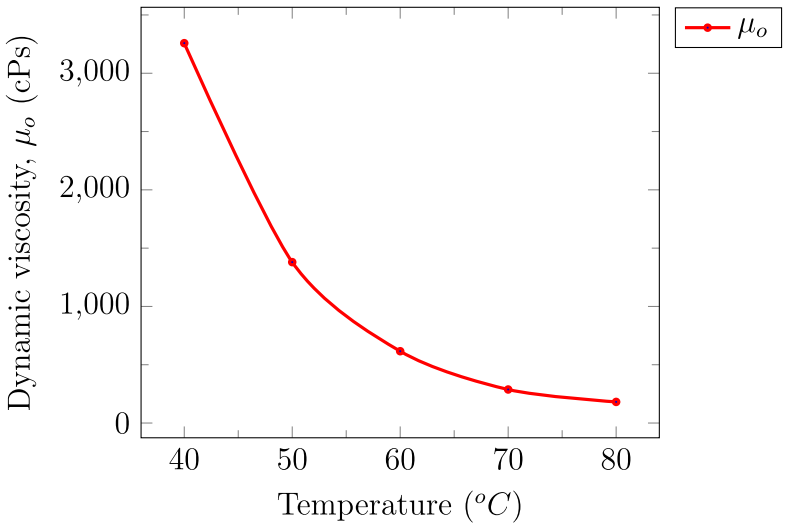

Fig. 4. Dynamic viscosity profile as a function of temperature for the heavy crude oil system used in this investigation.

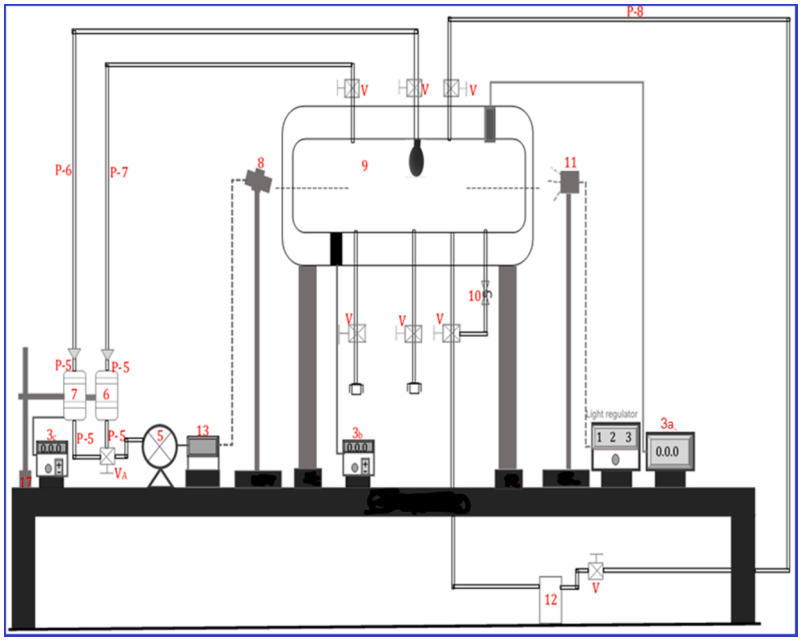

Fig. 5. Schematics of the developed HPHT IFT experimental set-up showing: tubing pipes (P5-P8); valves (V); digital indicators and regulators (items 3a, 3b and 3c); syringe pump (item 5); accumulators (items 6 and 7); video-camera (item 8); HPHT IFT-chamber (item 9); pressure relief valve device (item 10); illuminator (item 11); effluent tank (item 12); data acquisition system (item 13).

2.5.1. ST and IFT reduction analyses for brine and heavy crude oil system (unconfined measurements)

In order to measure the ST and IFT of the liquid–liquid and liquid–air phases, a Kruss K-6 tensiometer was used. First, the kit was calibrated with deionised water by taking surface-to-air measurements in triplicate to obtain an average reading of 72.2 dynes/cm (e.g. Heller et al. [32]). The surface activity of the SLs produced by *Meyerozyma* spp. MF138126 was then determined by making separate dilutions of the two supernatants obtained at 25 °C and 45 °C in a typical formation brine (composition in Table 2). Thereafter, a thin film of heavy crude oil was added onto the surface to create biosurfactant-brine and heavy crude oil interface. ST and IFT measurements of the samples were recorded at three different temperatures of 25, 45 and 65 °C. Briefly, a platinum ring is lowered into each of the solutions to be analysed until it is completely submerged. Upon pulling the ring vertically upward and out of the sample solution, the force that is required to ultimately break contact of the ring to the solution is measured.

Fig. 4 shows the dynamic viscosity profile as a function of temperature for the heavy crude oil system used in this investigation. Measurements were carried out by measuring dynamic viscosity and generating a profile created by cooling the sample from 80° down to as low as readings could be measured, using the Brookfield method (Intertek UK). For this sample, it is evident that the viscosity increases dramatically at around 40° and basically indicating why it was not possible to take measurements at 30° and below.

2.5.2. HPHT IFT experimental set-up

Fig. 5 shows the schematics of the special purpose HPHT IFT experimental set-up specially developed for the purpose of this investigation. The main component part of the set-up is the HPHT pendant drop chamber built by Sitec-Sieber Engineering and re-designed and re-fabricated in–house to measure the system IFT under varying

experimental pressure and temperature. The design pressure and temperature are 500 MPa (5000 bar) and 175 °C respectively. The chamber also has a unique customised dual-drop needle that allows for a phase to be dropped from the roof capillary-needle (for $\rho_d > \rho_e$) or from the bottom capillary-needle (for $\rho_d < \rho_e$) respectively. The HPHT chamber has two see-through windows coupled with a fixed Rame-Hart video-camera/frame grabber combination on one side and a light source (illuminator) on the other side (see Fig. 5). The video-camera is placed at a distance of 0.049 m (49 mm) from the fore-ground see-through window and the aspect ratio adjusted by calibration both in vertical and horizontal direction. The light source is tilted at an angle of 50 degrees for proper focus. The video image is an array of pixels each with 256 levels of light intensity (gray scale). The drop profile is detected using edge-tracing filter routine and the interface is detected using a local threshold and interpolation routine. The volume (v) and surface area (A) of the image are calculated using linear interpolation of the drop profile. The temperature of the IFT-chamber is controlled by a Type-J thermocouple fitted with a digital indicator. The pressure of the system is maintained externally through a syringe pump (maximum pressure of 82.7 MPa or 827 bar, Vindum).

2.5.3. ST and IFT reduction analyses for brine and heavy crude oil system (confined-chamber measurements)

In the current work, heavy crude-brine/SLs system has been taken as the reference fluid with brine or brine/SLs being the environmental phase/fluid and heavy crude the drop phase/fluid. The steps involved in the IFT measurement are as follows:

- The IFT-chamber is filled with the environmental fluid at a set pressure and injection rate of 0.01 $dm^3\ min^{-1}$ using an accumulator primed by a syringe pump. At all times, the pressure inside the IFT-chamber is maintained and the temperature set and maintained by a Type-J thermocouple connected to a heating controller.
- Once the IFT-chamber containing the environmental fluid has attained the required pressure and temperature, a pendant drop of the reference fluid (crude oil) is gradually created at a very low injection rate of 0.00002 $dm^3\ min^{-1}$ through a customised capillary drop needle system and regulated using a two-way stainless steel valve.
- As soon as the pendant drop is created, the camera and the DROP image software starts to capture the high-resolution digital images of the pendant drop for analysis.
- The density data of the reference fluid and density of environmental fluid were used as an input to the software to obtain the dynamic and equilibrium IFT of the heavy-crude/brine/SLs system.
- The fundamental principle involved in the calculation of IFT from the aforementioned measurement procedure is described below.

2.5.4. Specific conductance measurements

The specific conductances for the SLs in distilled water were measured by using a digital conductivity/TDS metre with a dip type conductivity cell from JENWAY, UK. It has an automatic temperature compensation of 1.91% per °C. In order to eliminate the variation in conductivity readings with temperature the samples were maintained at the reference temperature by using an equivalent of a thermostatic water bath. Before starting the measurements, the conductivity metre was calibrated by using a KCl solution of known conductivity as reference and the system equilibrated at an average temperature of 25 °C for at least 30 min.

2.6. Surface excess and thermodynamics of adsorption – brine-SLs

The concentration of SLs molecules in the surface plane relative to bulk phase (i.e. brine-SLs surface excess) is measured and used to analyse the behaviour of biosurfactants at the interface by Gibbs adsorption equation. From the concentration and surface tension data, the surface excess concentration (Γ_{min}) of SLs at their critical micelle concentration (CMC) was determined. The general form of the Gibbs [33] equation for a system at constant temperature can be written as:

$$d\gamma = -\sum_i \Gamma_i^{\sigma} d\mu_i \tag{7}$$

where, Γ_i^{σ} is the surface excess concentration of component i, γ is the ST or IFT, R is the universal gas constant, T is the temperature, μ_i is the chemical potential of component i which can be expressed as:

$$\mu_i = \mu_i^o + RT\ln a_i. \tag{8}$$

Differentiating Eq. 8 under constant temperature gives:

$$d\mu_i = RTd\ln a_i. \tag{9}$$

μ_i^o is the standard chemical potential of component i. Applying Eq. 9 to Eq. 7 gives the common form of the Gibbs equation for non-dissociating systems (e.g., non-ionic biosurfactants), thus:

$$d\gamma = -\Gamma_2^{\sigma} RTd\ln a_2, \tag{10}$$

which can also be written as:

$$\Gamma_2^{\sigma} = -\frac{1}{RT}\frac{d\gamma}{d\ln a_2}, \tag{11}$$

In the presence of dissociating solute, such as anionic surfactants of the form A^-B^+ and assuming ideal behaviour below the CMC, Eq. 10 becomes

$$d\gamma = -\Gamma_A^{\sigma} d\mu_A - \Gamma_B^{\sigma} d\mu_B, \tag{12}$$

If no electrolyte is present, electroneutrality of the interface will mean that $\Gamma_A = \Gamma_B$ and the Gibbs equation for a 1 : 1 dissociating compounds can be written as:

$$\Gamma_2^{\sigma} = -\frac{1}{2RT}\frac{d\gamma}{d\ln a_2}, \tag{13}$$

The following relations are then used to determine the minimum area per molecule of surfactant (A_{min}) and the free energy of micellisation per mole of a fully ionised SL surfactant.

$$A_{min} = \frac{10^{16}}{N_A \Gamma_{min}}, \tag{14}$$

$$\Delta G_m^0 = (1+\alpha)RT\ln X_{cmc}, \tag{15}$$

where,

$$\alpha = (1-\beta), \tag{16}$$

$$\beta = \frac{S_2}{S_1}, \tag{17}$$

α is the degree of counter-ion dissociation, X_{cmc} is the CMC of SLs biosurfactant in terms of its mole fraction in aqueous solution, β is degree of ionisation, S_1 and S_2 are the slopes of conductivity versus concentration plot for the pre- and post-micellar region respectively, ΔG_m^0 is the change in Gibbs free energy estimated at the CMC ($KJmol^{-1}$), R is the gas constant (8.314 J K^{-1} mol^{-1}), a is the activity which can be replaced by concentration c without loss of generality, N_A is the Avogadro's number ($= 6.022 \times 10^{23}\ mol^{-1}$), T is the temperature (298.15 K or 25 °C, 318.15 K or 45 °C and 338.15 K or 65 °C), and n is the sum of charge number of all ions resulted from the ionisation of the surfactant molecule (i.e. n = 1 for non-ionic surfactants and n = 2 or 3 for mono or

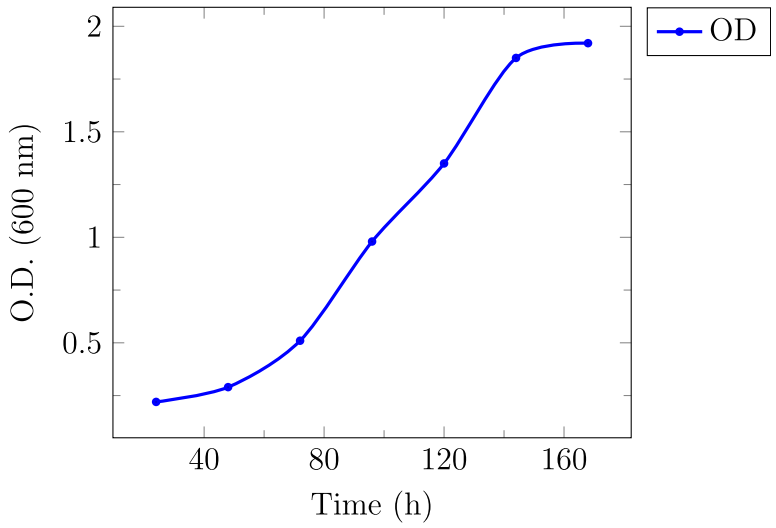

Fig. 6. Growth curve – optical density (O.D.) measurement versus time – for *Meyerozyma* spp. MF138126 during incubation under anaerobic ambient conditions.

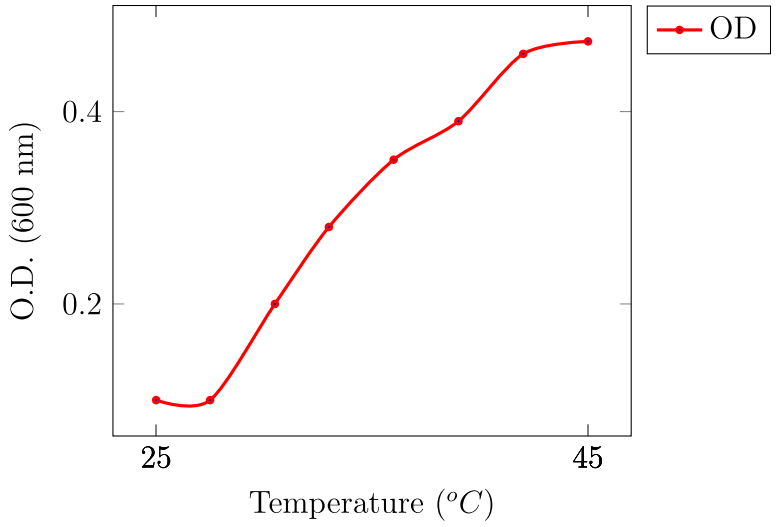

Fig. 7. Growth curve – optical density (O.D.) measurement versus temperature – for *Meyerozyma* spp. MF138126 under anaerobic high-pressure high-temperature conditions.

divalent counter ion, respectively).

3. Results and discussion

3.1. Anaerobic cultivation of Meyerozyma spp. MF138126 under ambient conditions

Meyerozyma spp. MF138126 was incubated under anaerobic ambient conditions. Fig. 6 shows the results of a typical growth curve post-incubation of one week. The yeast strain showed considerable growth as significant turbidity in the culture medium was observed even after 48 h of inoculation. It was noted that *Meyerozyma* spp. MF138126 harboured a lag phase of 48 h which was followed by a log phase of 96 h. Afterwards, a constant stationary phase was recorded during which no apparent increase in microbial growth was observed.

3.2. Anaerobic cultivation of Meyerozyma spp. MF138126 under HPHT conditions

Meyerozyma spp. MF138126 was subjected to different anaerobic HPHT conditions in the reactor chamber. Fig. 7 shows the results of a typical growth curve post-incubation of one week. Pressures of 1 bar and 10 bar were imposed on the reactor cell in a sequential experiment under two different temperatures (25 °C and 45 °C). Initially the culture density of 0.1 was recorded which increased considerably to 0.462 at the end of log phase, despite the increase in temperature from 25 to 45 °C. The biomass produced under HPHT conditions was comparatively lesser than that obtained in shake flasks fermentation cultivation conducted under ambient conditions. However, display of all the three phases of growth by *Meyerozyma* spp. MF138126 even under HPHT conditions showed the effective acclimatisation of the microorganism to the surrounding adverse environment. Moreover, a notable increase in cellular biomass even at high temperatures showed that the yeast strain can be

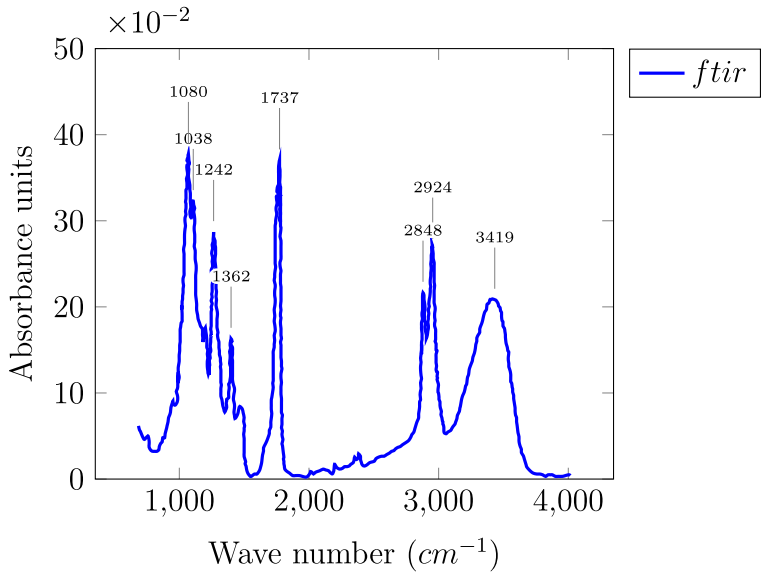

Fig. 8. FTIR spectrum of standard sophorolipids.

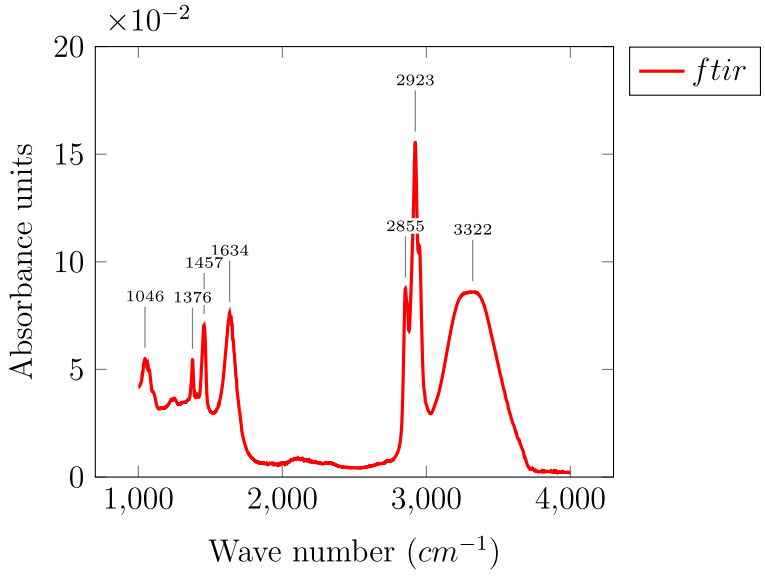

Fig. 9. FTIR spectrum of sophorolipids produced by *Meyerozyma* spp. MF138126 under HPHT conditions.

an effective cellular resource for insitu experimental conditions.

4. Application of SLs produced by *Meyerozyma* spp. MF138126 in interfacial phenomena

Surfactants can form oriented interfacial monolayers and aggregate to form micelles at sufficiently high concentration. The reduction in ST and IFT is achieved through the adsorption of surfactants micelles at the interface. A number of factors such as surfactant concentration, temperature, pH, salinity etc affect the rate of adsorption of the SLs at the interface. For this particular reason, the ST and IFT reduction was studied in a typical reservoir crude oil-formulation brine mixture for SLs produced by Meyerozyma spp. MF138126 under varying concentration, pressure, temperature and pH.

The supernatant obtained at 25 °C of incubation showed significant reduction in ST and IFT of the SLS-brine and heavy crude oil mixture at the three aforementioned temperatures of 25, 45 and 65 °C. It was observed that the pH of the mixture reduced with increasing concentration of sophorolipids. Similar was the case for ST and IFT. The least ST value of 14 mN/m was observed with the highest concentration of sophorolipids. IFT values when tested under the same temperature conditions showed that with increasing temperature, a continuous decline in brine-crude IFT in the presence of SLs manifests.

4.1. FTIR spectroscopic analysis of the SLs produced under HPHT conditions

Fig. 8 shows the standard SLs purchased from Sigma Aldrich and Fig. 9 shows the FTIR spectrum of crude SLs produced by *Meyerozyma* spp. MF138126 under HPHT conditions. It was noted that most of the peaks lie in the same spectrum for both samples. A broad band observed within the range of 3200–3500 cm^{-1} is due to the characteristic hydroxyl (O–H) stretch whereas, the two bands at 2923 and 2855 cm^{-1} represent the asymmetric and symmetric stretching of methylene groups (CH_2), respectively. The band at 1634 cm^{-1} corresponds to the stretching of unsaturated C = C linkage whereas the band at 1457 cm^{-1}

Table 3
Description of material properties.

Drop phase	Heavy crude oil
Environmental phase	Brine + SLs (biosurfactant)
Crude density, ρ_d (g-cm^{-3})	0.9985
Crude total acid number, TAN (mg KOH/g)	3.7
Crude total base number, TBN (mg KOH/g)	5.0
Asphaltene content (% m/m)	3.6
Brine + SLs density, ρ_e (g-cm^{-3})	1.027
Molecular weight of SLs (g-mol^{-1})	711
Acceleration due to gravity (m-s^{-2})	9.81
Stock brine concentration (mg/L)	0.50958

is the C-O-H group in the plane bending of carboxylic moiety in SLs. Moreover, the carbonyl stretch C-O of lactonic SLs was observed at 1046 cm^{-1}. This structural analysis of SLs produced by *Meyerozyma* spp. MF138126 under HPHT conditions is also in accordance with the previous reports of Bajaj and Annapure [34], Sheshtawy et al. [35] and Jiménez-Peñalver et al. [36].

The current findings suggest that the produced SLs is not only effective under ambient conditions but also under HPHT in unconfined systems. Moreover, the molecular integrity of SLs was retained even at this elevated conditions considered to be a harsh environment.

4.2. ST and IFT reduction analyses

The results of the unconfined and confined-chamber measurements are presented in this section. Table 3 shows the summary of the material properties associated with ST and IFT measurements for the unconfined and confined-chamber experiments.

4.2.1. ST and IFT reduction analyses for unconfined measurements

Figs. 10 and 11 show the effect of SLs concentration on ST and IFT of the crude oil-brine system. For this purpose, 2–20 vol.% concentrated solutions of SLs were prepared. Initially, the ST of brine-SLs mixture was recorded then IFT of the crude oil-brine/SLs systems. It was observed that with an increase in concentration, the ST of brine solution decreased continuously till 12 vol.% (0.17 mM) concentration of SLs. After this point, a constant ST value of 14 mN/m was recorded which

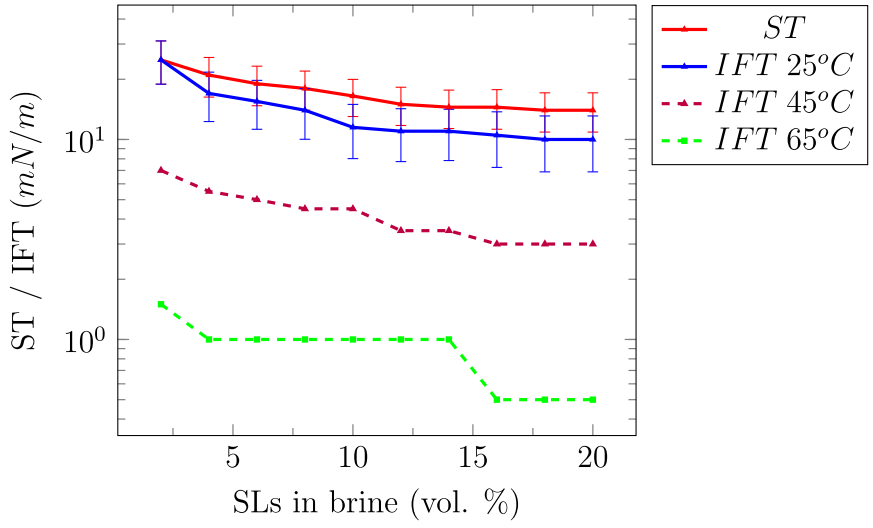

Fig. 10. Equilibrium ST and IFT for sophrolipids produced from *Meyerozyma* spp. MF138126 at 25 °C. The experiments were carried out using the aqueous solution of SLs in brine with heavy crude-oil at different temperatures.

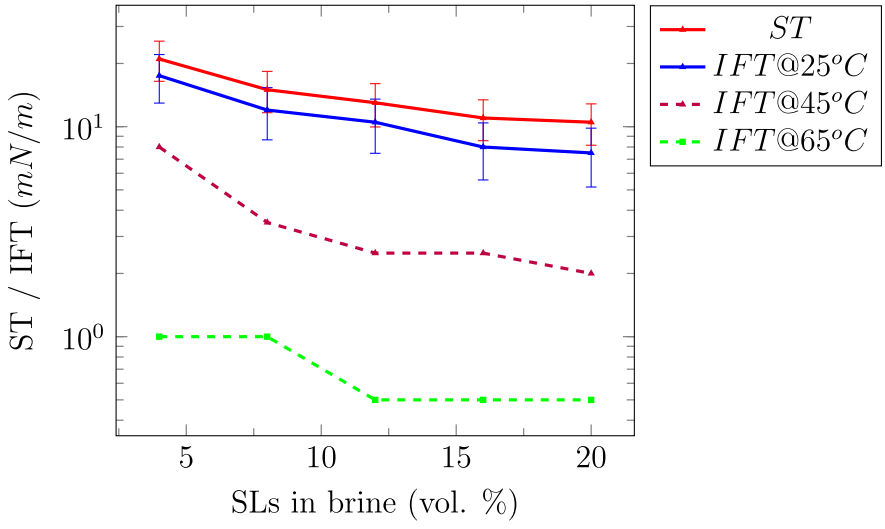

Fig. 11. Equilibrium ST and IFT for sophorolipids produced from *Meyerozyma* spp. MF138126 at 45 °C. The experiments were carried out using the aqueous solution of SLs in brine with heavy crude-oil at different temperatures.

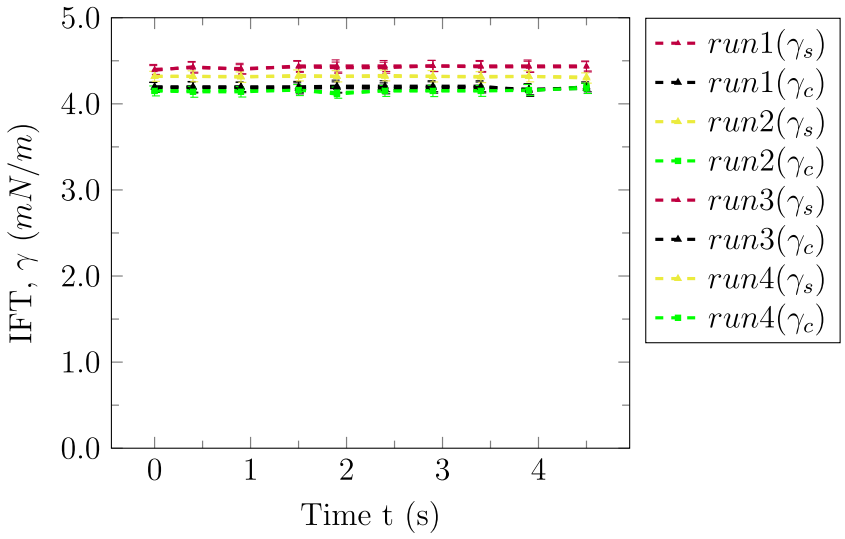

Fig. 12. Validation results for a typical confined-chamber IFT experiments conducted at a pressure of 1 bar and temperature of 25 °C. γ_c is the IFT values obtained from analytical calculations and γ_s is the DROPImage IFT values.

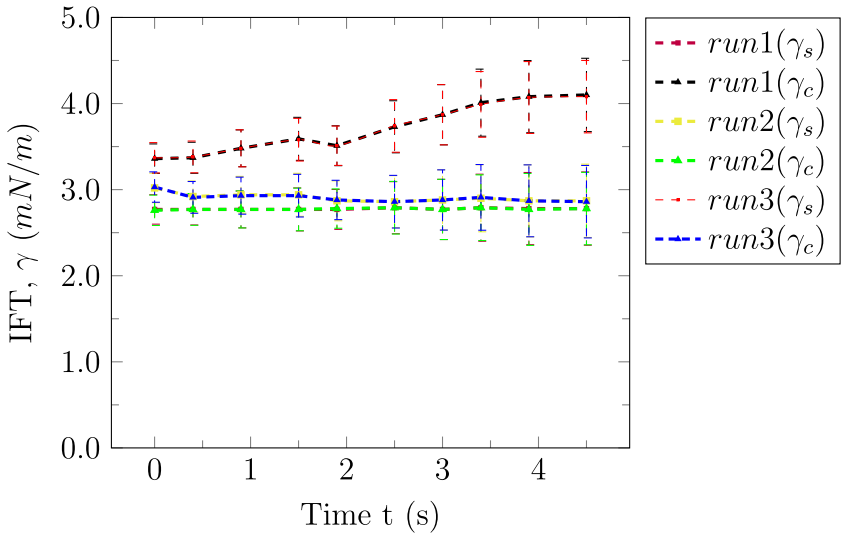

Fig. 13. Validation results for a typical confined-chamber IFT experiments conducted at a pressure of 25 bar and temperature of 25 °C. γ_c is the IFT values obtained from analytical calculations and γ_s is the DROPImage IFT values.

remained constant up to 20 vol.% (0.28 mM) concentration of SLs in brine formulation. Similarly, a linear increase in SLs concentrations resulted in reduction of IFT for crude oil-SLs-brine system. The IFT value decreased from 25 mN/m to 11 mN/m at 12% SLs concentration and 25 °C, after which it remained almost constant. However, with similar concentration, the IFT value further decreased up to the point of 3 mN/m and 0.5 mN/m when the temperature was elevated to 45 °C and 65 °C, respectively. The mean, standard deviation and standard error of all the measurements are stated in Tables SA.1–SB.2 (Appendix A–B). This result demonstrates, for the very first time, that SLs not only significantly reduced the ST and IFT of the COBBIO system but that it does so at a very low concentration of 12 vol.% (0.17 mM).

4.2.2. ST and IFT reduction analyses for confined-chamber measurements

For the confined-chamber measurements, each experimental run was repeated at least three times under a fixed pressure and temperature with ten computational points generated for all the constitutive variables highlighted in Section 2.4. Tables SD.4–SD.14 of Appendix D show the results of the data generated for the HPHT IFT measurements between the environmental phase (brine plus SLs) and the drop-phase (heavy crude-oil) at different pressures of 1 to 80 bar and fixed temperature of 25 °C.

In order to validate the obtained dataset, analytical calculations were carried-out for the IFT values (γ_c) and compared with those obtained from the DROPImage software (γ_s). Figs. 12 and 13 show the validation results for the IFT versus time at pressures of 1 and 25 bar. Both values (γ_c and γ_s) were exactly the same for almost all the 10 points generated for each run at equilibrium; with a minimum and maximum error of 0.02% and 0.52% for 1 bar and 0.01% and 0.41% for 25 bar respectively. Similar profile was obtained in all the repeat-runs (Figs. 12 and 13).

Biosurfactants produced by isolated microorganisms have been reported to reduce the IFT between oil and water to 10 mNm^{-1} [37] or values slightly less than 10 mNm^{-1} for improved oil recovery process [38]; albeit, under unconfined low-pressure conditions. Fig. 14 shows the variation of IFT as a function of pressure at a fixed temperature of 25 °C in a confined-chamber system. Under confinement, the IFT of the COBBIO system (heavy crude oil/brine/SLs aqueous) at a pressure of 1 bar was 4.27 mN/m; reducing significantly to 0.251 mN/m when the

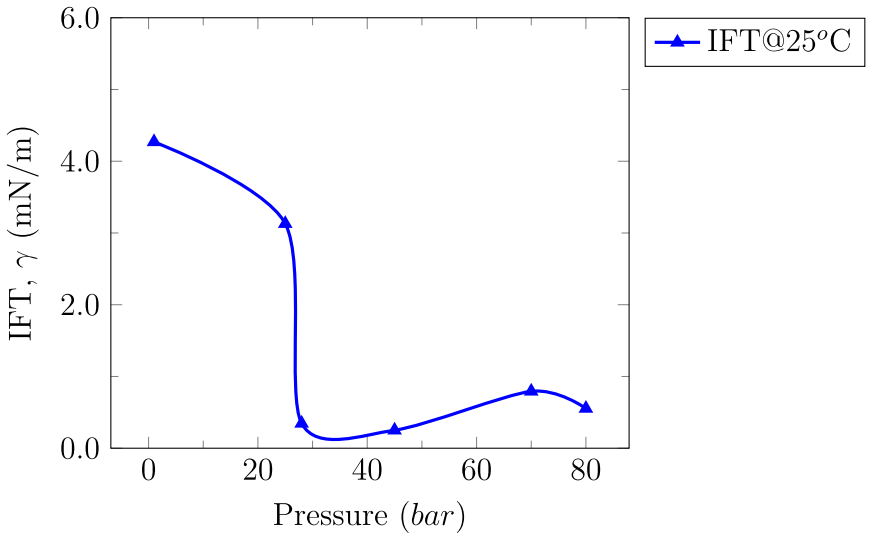

Fig. 14. Equilibrium IFT for brine/SLs – heavy crude systems at a fixed temperature of 25 °C and pressures of 1–80 bar.

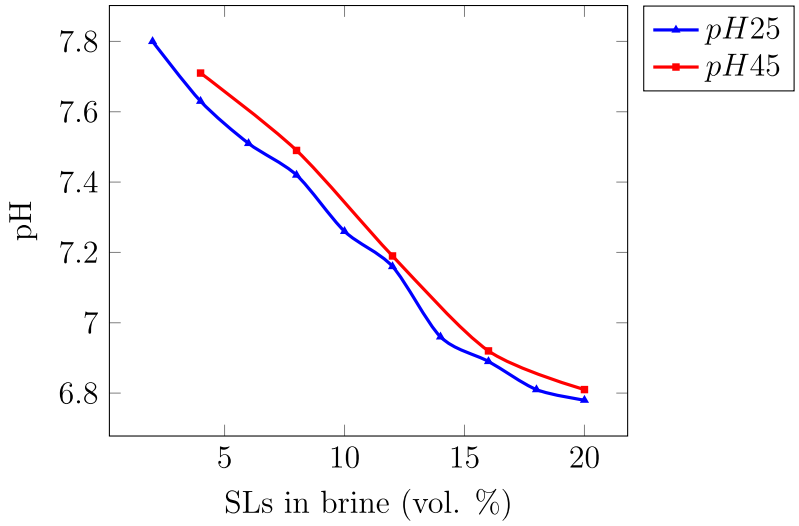

Fig. 15. pH as a function of sophorolipids concentration for anaerobic microbial fermentation at 25 °C and 45 °C respectively.

pressure was gradually increased to 45 bar at the same temperature of 25 °C. Increase in pressure basically caused the molecules of SLs to become more active in breaking the binding force between the crude oil and the brine, thereby, accelerating the rate of IFT reduction. The IFT value obtained at 1 bar under confined-chamber experiment (i.e. 4.27 mN/m) is significantly lower when compared with the value obtained under unconfined measurements (i.e. 25 mN/m) at the same temperature of 25 °C; despite the fact that the concentration was more than three orders of magnitude less in the confined experiments. This suggests that the effectiveness of SLs in reducing IFT is amplified under elevated or insitu pressure; making SLs a promising biosurfactant for EOR projects. Economic viability of SLs in EOR applications will be evaluated as part of separate investigation involving crude oil/brine/biosurfactant/rock (COBBIOR) system.

4.3. Effect of temperature on IFT of the system

IFT reduction studies were conducted at 25, 45 and 65 °C using different concentrations of SLs produced by *Meyerozyma* spp. MF138126. In the first set of experiments, the supernatant obtained from microbial culture incubated at 25 °C was used and IFT values ranging between 0.5 and 25 mN/m were recorded. Figs. 10 and 11 show a significant decline in IFT of SLS-brine and crude oil with temperature.

Elevated temperature enhances the solubility of solvents and favours the formation of water-in-oil emulsions rather than oil-in-water emulsions [39]. This inversion of phases facilitates the adsorption of surfactant monomers and eventually reduction of IFT. Mirchi et al. [40] stated that high temperature increases the kinetic energy and reduces the attractive forces between molecules. This also causes a decrease in IFT of the solution and oil.

4.4. Effect of pH on IFT of the system

pH of the brine-SLs mixture was monitored with varying biosurfactants concentration. Results (Fig. 15) shows a decrease in pH from 7.8 to 6.78 at 25 °C anaerobic fermentation when the SLs concentration was increased from 2% to 20%; and from 7.71 to 6.81 at 45 °C anaerobic fermentation when the SLs concentration was increased from 2% to 20%, respectively. The impact of fermentation temperature on the system pH is also observed as part of this analysis (see Fig. 15). pH plays a very important role in surfactants adsorption on liquid–liquid and liquid-rock surfaces for anionic surfactants. see Fig. 16,17.

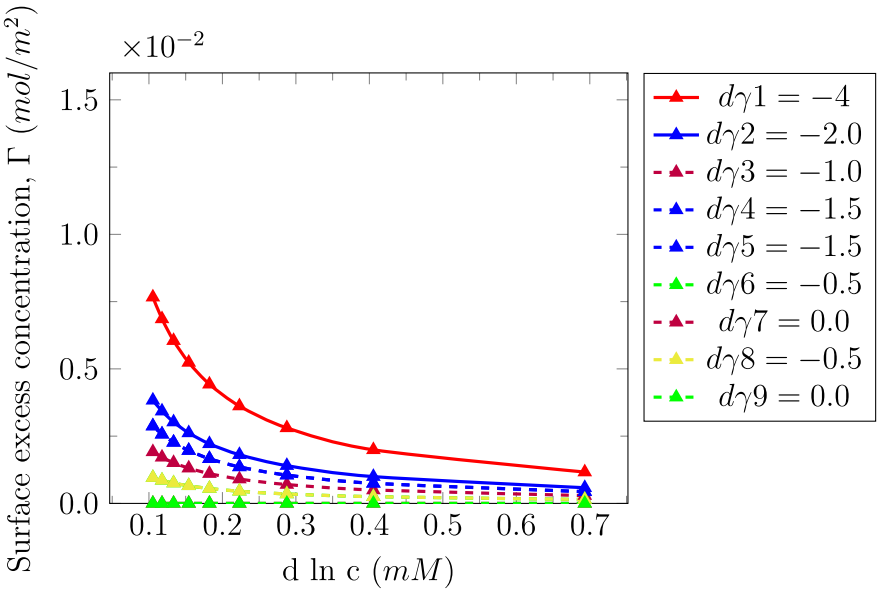

Fig. 16. Surface excess concentration (mol/m^2) versus d ln$c$ for different values of dγ – ST measurements at 25 °C and microbial fermentation at 25 °C.

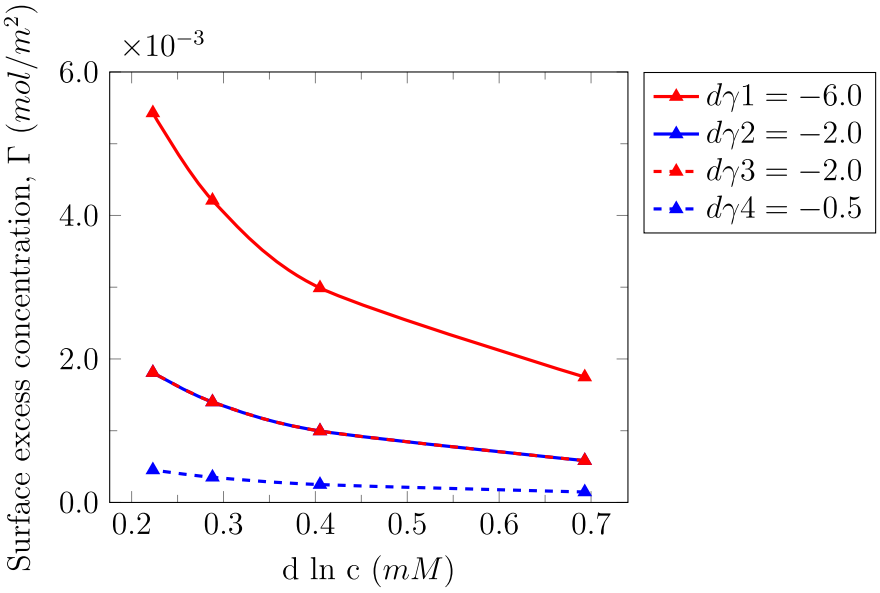

Fig. 17. Surface excess concentration (mol/m^2) versus d ln$c$ for different values of dγ – ST measurements at 25 °C and microbial fermentation at 45 °C.

4.5. Analysis of thermodynamic properties

Figs. 18–23 show graphs of surface excess concentration Γ (mol/m^2) versus the change in ln$c$ (i.e. dln$c$) for different values of γ (i.e. dγ). Both cases of ST and IFT measurements at 25 °C, 45 °C, 65 °C and microbial fermentation of both 25 °C and 45 °C, were investigated respectively.

The surface excess concentration, Γ provides a direct information about the interaction of the molecules of SLs and the other phases at an interface when a brine is enriched at that interface. The observed reduction in surface tension when the solution concentration is increased indicates that SLs is a surface active agent. The analysis conducted in this study further revealed the fact that the Γ not only reduced with increase in change in ln$c$ (i.e. dln$c$), but, the profile of the plots changes depending on the values of γ (i.e. dγ) which is also implicitly dependent on concentration. This can be seen in a typical graphical plot (e.g. Fig. 18). The effect of temperature on the surface excess concentration can also be seen in Figs. 18–20 for the microbial fermentation temperature of 25 °C and Figs. 21–23 for the microbial fermentation temperature of 45 °C. As the temperature increases, the degree of SLs adsorption at the interface increases leading to a collapse in the trends of the Γ. Table 4 indicates the minimum area per molecule of SLs for the different experimental and cultivation temperatures investigated in this study. It shows that when SLs was added, the interface weakens occupying more surface area as the temperature increases. This observation is in line with Kosaka et al. [41]. The degree of counter-ion binding for SLs was obtained to be 0.86. The computed Gibbs free energy of

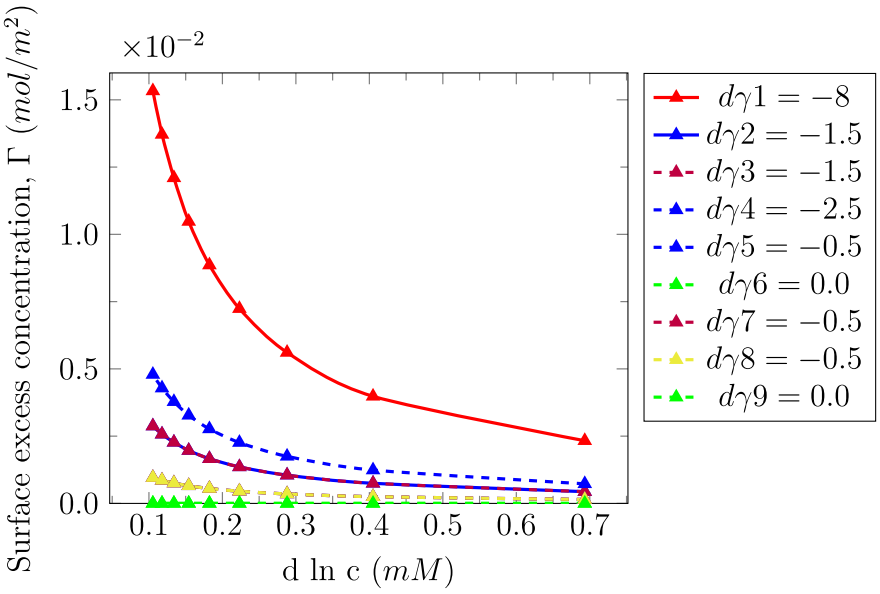

Fig. 18. Surface excess concentration (mol/m^2) versus d ln$c$ for different values of dγ – IFT measurements at 25 °C and microbial fermentation at 25 °C.

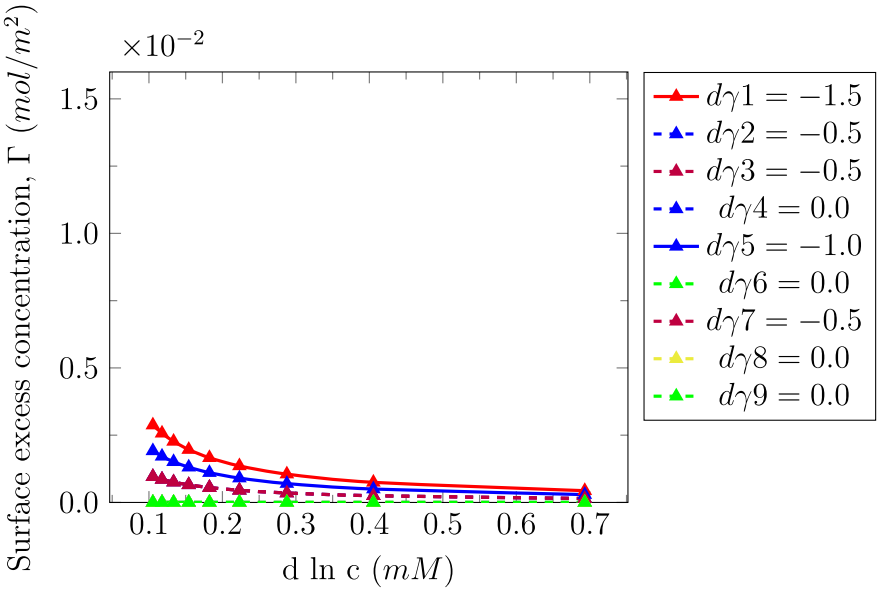

Fig. 19. Surface excess concentration (mol/m^2) versus d ln$c$ for different values of dγ – IFT measurements at 45 °C and microbial fermentation at 25 °C.

micellisation is −1940 KJmol^{-1} (i.e. $\Delta G < 0$) which is exergonic depicting favourable reaction and spontaneous in forward direction. Process reactions are endergonic and unfavourable when $\Delta G > 0$ and energy is absorbed.

4.6. Specific conductance in the bulk

The specific conductance, κ, of the different surfactant solutions is plotted in Fig. 24. Each plot shows that conductivity linearly correlated with the surfactant concentration in the pre-micellar and post-micellar regions. The intersection between two straight lines gives the break point, and hence cmc value. The cmc values obtained from κ measurements is 3.703 × 10^{-3} mol/L.

5. Conclusions

A novel technique for interface behaviour and thermodynamic properties analyses of biosurfactant is developed. The micellisation behaviour and thermodynamic properties of SLs obtained from *Meyerozyma* spp. MF138126 under HPHT for low-salinity heavy-crude experiments is studied. The new environmentally benign microbial strain was previously isolated from a crude oil contaminated site and screened for its SLs producing capabilities.

- A series of anaerobic fermentation experiments under HPHT conditions in a reactor chamber is conducted. Samples are collected periodically under varying conditions of temperature and pressure to

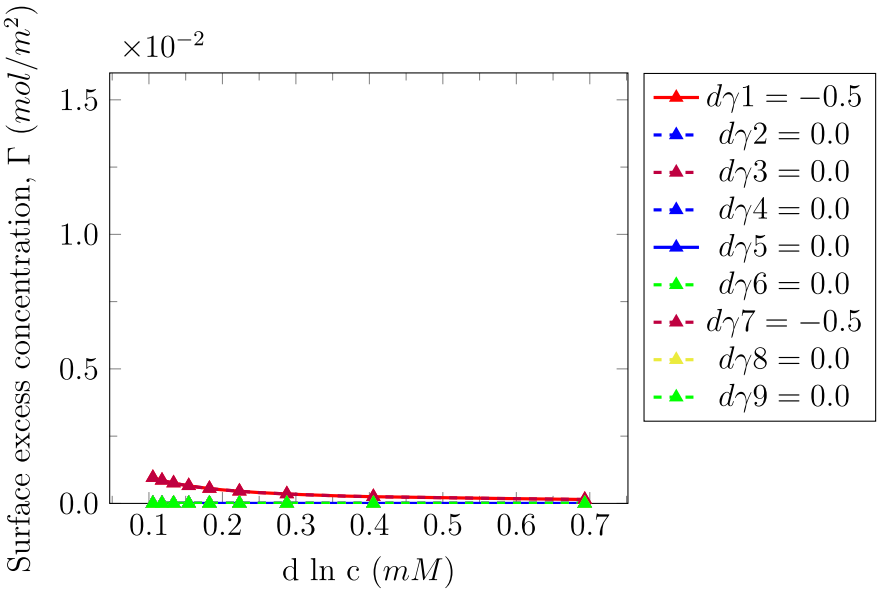

Fig. 20. Surface excess concentration (mol/m^2) versus d ln$c$ for different values of dγ – IFT measurements at 65 °C and microbial fermentation at 25 °C.

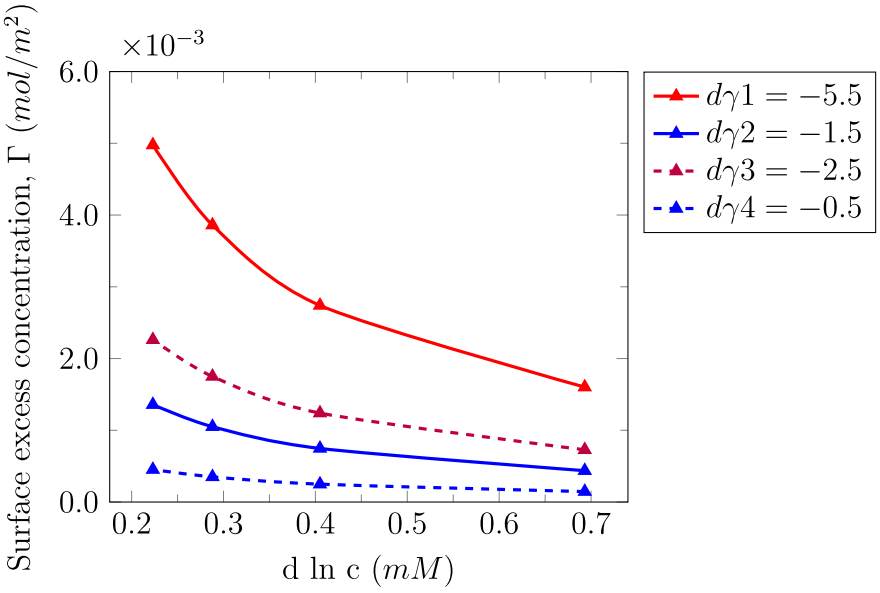

Fig. 21. Surface excess concentration (mol/m^2) versus d ln$c$ for different values of dγ – IFT measurements at 25 °C and microbial fermentation at 45 °C.

monitor growth-rate and produced cellular biomass using spectrophotometer.

- We report for the very first time, the potential of the isolated strain and the produced SLs to reduce IFT between the formulated low salinity formation brine and heavy crude by up to a factor of five (5) and seven (7) for the anaerobic cultivation of 25 °C and 45 °C respectively. Increasing experimental temperature to 45 °C and 65 °C brings about a reduction of a factor of seven (7) and nine (9) in IFT respectively.
- From the ST results, it can further be concluded that the packing of SLs monomers at brine/SLs and SLs/crude oil interfaces becomes loose at high temperature.
- Furthermore, using surface tensiometry, the CMC, the thermodynamics of adsorption, surface excess concentration and the minimum area occupied by surfactant monomers were determined. The degree of counter-ion binding for SLs is obtained to be 0.86. The computed Gibbs free energy of micellisation is −1940 kJ/mol; which is

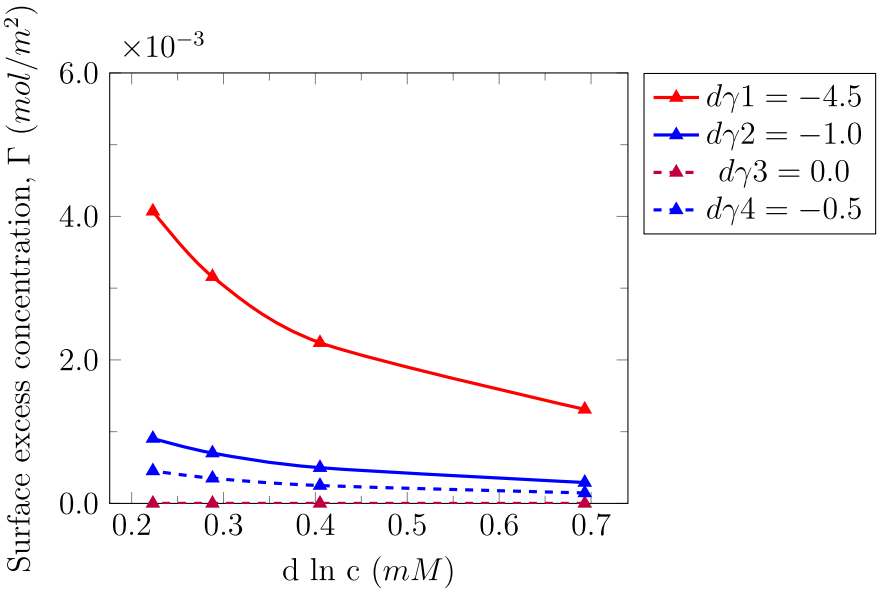

Fig. 22. Surface excess concentration (mol/m^2) versus d ln$c$ for different values of dγ – IFT measurements at 45 °C and microbial fermentation at 45 °C.

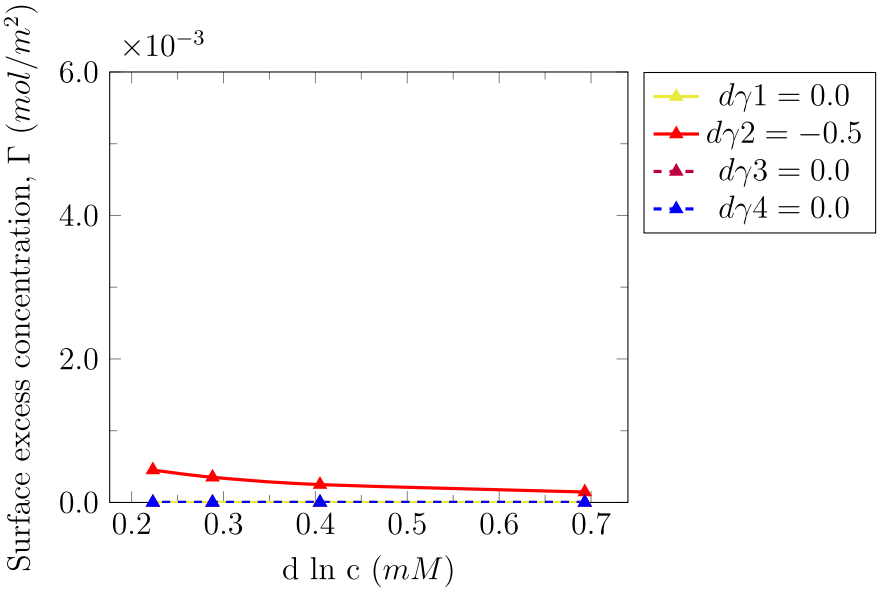

Fig. 23. Surface excess concentration (mol/m^2) versus d ln$c$ for different values of dγ – IFT measurements at 65 °C and microbial fermentation at 45 °C.

Table 4
Minimum area per molecule of sophorolipids biosurfactant A_{min} (cm^2) at different measurement and anaerobic fermentation temperatures.

	ST	IFT		
	25 °C	25 °C	45 °C	65 °C
25 °C anaerobic fermentation	1.43E−05	7.13E−06	3.80E−05	0.00011
45 °C anaerobic fermentation	9.50E−06	3.80E−05	1.27E−05	0.00011

exergonic depicting favourable reaction and spontaneous in forward direction.

- IFT value of 0.251 mN/m was obtained at an elevated pressure of 45 bar. Similarly, keeping the temperature constant at 25 °C and increasing the pressure up to 80 bar, the IFT reduces. It is concluded that the produced SLs retained its molecular integrity and effectiveness under unconfined ambient conditions with an amplified activity under HPHT confined systems.

Declaration of Competing Interest

The authors declare that they have no known competing financial interests or personal relationships that could have appeared to influence

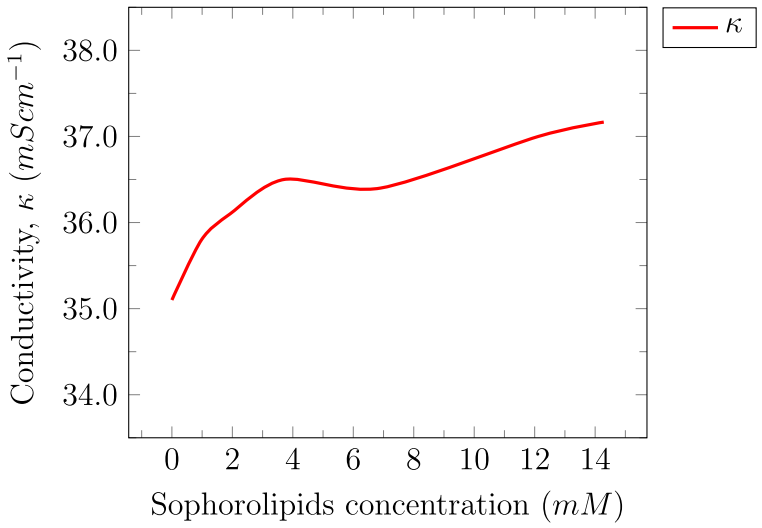

Fig. 24. The plot of specific conductivity versus concentration of sophorolipids at 25 °C (1 mM $= 10^{-3}$ mol/L).

the work reported in this paper.

Appendix A. Supplementary data

Supplementary data associated with this article can be found, in the online version, athttps://doi.org/10.1016/j.fuel.2021.120607.

References

[1] Tadros TF. Wiley-VCH, Weinheim; 2005.
[2] Koh A, Wong A, Quinteros A, Desplat C, Gross R. In uence of sophorolipid structure on interfacial properties of aqueous-arabian light crude and related constituent emulsions. J Am Oil Chem 2017;94:107–19.
[3] Bollmann T, Zerhusen C, Glüsen B, Schörken U. Structures and properties of sophorolipids in dependence of microbial strain, lipid substrate and post-modification. J Am Oil Chem 2019;56:367–77.
[4] Wang X, Lin R, Gross R. Sophorolipid butyl ester: an antimicrobial stabilizer of essential oil-based emulsions and interactions with chitosan and γ-poly (glutamic acid). ACS Appl Bio Mater 2020;3:5136–47.
[5] Kiran GS, Thomas TA, Selvin J, Sabarathnama B, Lipton AP. Optimization and characterization of a new lipopeptide biosurfactant produced by marine brevibacterium aureum msa13 in solid state culture. Bioresour Technol 2010;101:2389–96.
[6] Ramos GAR, Akanji LT, Afzal W. A novel surfactant-polymer/alkaline-surfactant-polymer formulation for enhanced oil recovery (eor) processes. Energy Fuels 2019:-.
[7] Desai JD, Banat IM. Microbial production of surfactants and their commercial potential. Microbiol Mol Biol Rev 1997;61:47–64.
[8] Al-Sulaimani H, Al-Wahaibi Y, Al-Bahry A, Elshafie S, Al-Bemani A, Joshi S, Zargari S. Optimization and partial characterization of bio657 surfactants produced by bacillus species and their potential for ex-situ enhanced oil recovery. Soc Petrol Eng 2011.
[9] Chisholm J, Kashikar S, Knapp R, McInerney M, Menzie D. Microbial enhanced oil recovery: interfacial tension and gas-induced relative permeability effects, 20481; 1990.
[10] Budiharjo A, Jeong H, Wulandari D, Lee S, Ryu CM. Complete genome sequence of bacillus altitudinis p-10, a potential bioprotectant against xanthomonas oryzae pv. oryzae, isolated from rice rhizosphere in java, Indonesia. Genome Announcement 2017;5.
[11] Poremba K, Gunkel W, Lang S, Wagner F. Toxicity testing of synthetic and biogenic surfactants on marine microorganisms. Environ Toxicol Water Qual 1991;6:157–63.
[12] Norde W. Driving forces for protein adsorption at solid surfaces. Macromol Symposia 1996;103:5–18.
[13] Nakanishi K, Sakiyama T, Imamura K. On the adsorption of proteins on solid surfaces, a common but very complicated phenomenon. J Biosci Bioeng 2001;91:233–44.
[14] Rosen MJ. Adsorption of surface-active agents at interfaces: the elec675 trical double layer. 3rd Ed.; 2004.
[15] Al-Wahaibi Y, Joshi S, Al-Bahry S, Elshafie A, Al-Bemani A, Shibula B. Biosurfactant production by bacillus subtilis b30 and its application in enhancing oil recovery, vol. 114; 2014.
[16] Al-Araji L, Rahman R, Basri M, Salleh A. Microbial surfactant. Asia Pac J Mol Biol Biotechnol 2007;15:99–105.
[17] Anitha J, Jeyanthi P, Ganesh V. Production and characterization of biosurfactant by bacillus and its applicability in enhanced oil recov ery. Int J Adv Res Biol Sci 2:2015; 716.
[18] Speight JG. Marcel Dekker Inc.; 1991.
[19] Lanier D. Heavy oil – a major energy source for the 21st century. Technical Report 039, UNITAR Centre for heavy crude and tar sands; 1998.
[20] Keomany D, Asnachinda E. Adsorption and adsolubilization of organic solutes using rhamnolipid biosurfactant modified surface. In: 1st Environment and natural resources international conference, Thailand; 2014. p. 231–6.
[21] Camargo FP, Menezes AJ, Tonello PS, Dos Santos ACA, Duarte ICS. Characterization of biosurfactant from yeast using residual soy bean oil under acidic conditions and their use in metal removal processes. FEMS Microbiol Lett 2018;365. fny098.
[22] Camargo FP, PPFD, Tonello PS, Dos Santos ACA, Duarte ICS. Bioleaching of toxic metals from sewage sludge by co-inoculation of acidithiobacillus and the biosurfactant-producing yeast meyerozyma guilliermondii. J Environ Manage 211:2018; 28– 35.
[23] Liang X, SR, RM, Zhao F, Zhang Y, Han S, Zhang Y. Anaerobic lipopeptide biosurfactant production by an engineered bacterial strain for in situ microbial enhanced oil recovery. Roy Soc Chem 7: 2017; 20667–20676.
[24] Ganji Z, Beheshti-Maal K, Massah A, Emami-Karvani Z. A novel sophorolipid-producing candida keroseneae gbme-iauf-2 as a potential agent in microbial enhanced oil recovery (meor). FEMS Microbiol Lett 2020;367.
[25] Elshafie A, Joshi S, Al-Wahaibi Y, Al-Bemani A, Al-Bahry S, Al- Maqbali D, Banat I. Sophorolipids production by candida bombicola atcc 22214 and its potential application in microbial enhanced oil recovery. FEMS Microbiol Lett 2015;6:1324.
[26] Bagalkot N, Hamouda A, Isdahl O. Dynamic interfacial tension measurement method using axisymmetric drop shape analysis. MethodsX 2018;5:676–83.
[27] Amirianshoja T, Junin R, Kamal Idris A, Rahmani O. A comparative study of surfactant adsorption by clay minerals. J Petrol Sci Eng 2013;101:21–7.
[28] Barati-Harooni A, Najafi-Marghmaleki A, Tatar A, Mohammadi AH. Experimental and modeling studies on adsorption of a nonionic surfactant on sandstone minerals in enhanced oil recovery process with surfactant flooding. J Mol Liq 2016;220:1022–32.
[29] Rehman R, Ali MI, Qureshi U, Jamal A. Characterization of brownfield: ex-situ detection of hydrocarbon degrading and biosurfac726 tants producing micro ora. Pak J Agric Sci 2019;56:953–61.
[30] Onyemara CC, Akanji LT, Ebel R. Development of a new high pressure high-temperature technology for advanced screening of biosurfactants and injection of microbes in porous rocks during low-salinity eor processes. In: Artificial intelligence, big data and mobile technology: changing the future of the energy industry; 2019. p. 26. doi.
[31] F.K. Hansen, Dropimage advanced – a program for the measurement of interfacial tension and contact angles by image analysis, http://www.ramehart.com/dropimagefinn.htm, 2006. Accessed: 2020-01-15.
[32] Heller W, Cheng M-H, Greene BW. Surface tension measurements by means of the "microcone tensiometer". J Colloid Interface Sci 1966;22:179–94.
[33] Gibbs JW. The collected works of J.W. Gibbs, vol. I. Longmans, Green, New York; 1931.
[34] Bajaj V, Annapure US. Castor oil as secondary carbon source for production of sophorolipids using starmerella bombicola. Oleo Sci 2015;64:315–23.
[35] El-Sheshtawy H, Aiad I, Osman M, Abo-ELnasr A, Kobisy AS. Production of biosurfactants by bacillus licheniformis and candida albicans for application in microbial enhanced oil recovery. Egypt Petrol 2016;25:293–8.
[36] Jiménez-Peñalver P, Gea T, Sánchez A, Font X. Production of sophorolipids from winterization oil cake by solid-state fermentation: optimization, monitoring and effect of mixing. Biochem Eng 2016;115:93–100.
[37] Parkinson M. Biosurfactants. Biotechnology 1985;3:65–83.

[38] McInerney MJ, Javaheri M, Nagle DP. Properties of the biosurfactant produced bybacillus licheniformis strain jf-2. J Ind Microbiol 1990;5:95–101.
[39] Ye Z, Zhang F, Han L, Luo P, Yang J, Chen H. The effect of temperature on the interfacial tension between crude oil and gemini surfactant solution. Colloids Surfaces Physicochem Eng As760 pects 2008;322:138–41.
[40] Mirchi V, Saraji S, Goual L, Piri M. Dynamic interfacial tension and wettability of shale in the presence of surfactants at reservoir conditions. Fuel 2015;148:127–38.
[41] Kosaka O, Sehgal P, Doe H. Behavior of cationic surfactants micellar 765 solution solubilizing an endocrine disruptor bisphenol a. Food Hydro Colloids 2008;22: 144–9.